Simulation of PVD for Coating of Tantalum Carbide on 316L SS Substrates

Siddu Anilkumar Pujari[1], Bharatish A[1*]

[1] *Department of Mechanical Engineering, RV College of Engineering, Bengaluru -560059*

Abstract

Tantalum Carbide has attracted the attention of medical research for enhancing the durability of implants. This paper presents simulation of depositing Tantalum carbide on 316L stainless steel using physical vapor deposition (PVD) process. Effect of PVD parameters such as vacuum pressure, Argon gas velocity and stand-off-distance on mass concentration and turbulence kinetic energy of Argon gas in a sputtering chamber, was studied. Optimal vacuum pressure, Argon gas velocity and stand-off-distance were 0.41Pa, 3.4 mm/s and 10 mm respectively.

Key words: *Tantalum Carbide, Physical Vapour Deposition (PVD), Simulation*

1.0 Introduction

Growing need for minimally invasive surgical treatments is expected to propel the medical coatings industry. Titanium nitride (TiN) is widely reported as a biocompatible material. Stainless steel (SS) alloys are traditional materials for surgical tools due to their high corrosion resistance and hardness. PVD coatings are commonly used in medical implant applications, electronics, energy, automotive, semiconductor industry, optical and ornamental applications. PVD coatings offer several benefits to medical devices in addition to toughness and adhesion.

Kapopara et al. [1] studied the mixing behavior of process gases in the deposition chamber based on three-dimensional computational fluid dynamics (CFD) analysis using Fluent-ANSYS. The findings indicated that placement of the gas inlet port has significant impact on the gas distribution within the chamber where the reactive gas develops coating. M. Venkata et al. [2] developed 3D model of prosthetic knee implants to analyze the stresses and deformations. Femur made of Co-Cr alloy, Ti alloy, SS, and zirconium oxide (ZrO_2) were analyzed. M. Zhang et al. [3] investigated flow and mechanical properties of porous Ti implant architectures. The models were evaluated to study the complicated

**Mail address: Bharatish A, Assistant Professor, Department of Mechanical Engineering, RV College of Engineering®, Bengaluru -560059*
Email: bharatisha@rvce.edu.in Ph: 988644503

relationships amongst load, fluid flow, and changes in porosity due to internal growth for implant design. Andresa Baptista et al. [4] reported applicability of FEA and CFD for PVD. While FEA helps to study substrate and coating, CFD is useful to examine gas structures and fluid flow. Francisco J et al. [5] reported that Zirconium nitride (ZrN) coating in hard surfaces is greatly influenced by coating adhesion, defects and density of coating.

PVD coating of ZrN find applications in rust-resistant clothing. PVD is widely regarded as advanced coating method for multifunctional and multilayer coatings [6-7]. Hiroaki Kitajima et al, [8] used CFD for fibrinogen and blood plasma penetration surrounding a dental implant. The study suggested that hydrophilic implant's surface can selectively remove fibrinogen from blood plasma to the area closest to the interface. Vicky Varghese et al. [9] studied biocompatible implant materials such as cobalt-chromium (Co-Cr), type 316 low carbon SS (316L SS), titanium alloy (Ti_6Al_4V), magnesium alloy (AZ91), carbon fiber reinforced PEEK, and carbon fiber reinforced PA-12. The implants were modelled and analyzed using ANSYS.

Rodianah Alias et al. [10] investigated thin multiple layers of TaO and Ag of thickness 4.7 to 6.4 µm respectively on SS 316L. Magnetron sputtering was used to deposit the multilayer thin-film coatings. Thin film of Ag / $AgTa_2O_5$ nanocomposite was fabricated for limiting bacterial attachment to surgical instrument. Kobayashi et al. [11] analyzed a 2-D model for reactive sputtering. Passage of N_2 gas from the intake to the target and the walls were observed. TiN film on the vast area substrate had a composition distribution. Daisuke Nakamura et al. [12] investigated a technique for producing ultra-thick (50 - 200 µm) protective coatings of TaC. The sintered TaC layers exhibit thick granular structure with coarse grains of 10 to 50 m. Jaydeep M. Kapoparaa et al. [13] analysed velocity profiles, pressure profiles, density profiles, and concentration distribution of process gas species (argon and nitrogen) via the spray chamber, a 3-D CFD study was conducted. The numerical predictions helped to understand the multi-species process gas distribution and mixing behaviour in the spray chamber at various gas flow rates. G. Pinto et al. [14] reported a vacuum reactor, the transition of atomic particles between the target and the parts to be coated is generally aided by plasma, which creates a special atmosphere at low pressure and medium temperature that is responsible for the transition of atomic particles between the target and the parts to be coated by using numerical simulations like CFD technique. H. Fouad et al. [15] developed ANSYS code to create 3D FEM of the SG material femoral head as well as

traditional SS, cobalt-chromium alloy (Co Cr Mo), and titanium alloy (Ti) femoral heads to imply that slight modifications in design and geometry characteristics of the hip joint have significant long-term repercussions and should be considered while developing the hip joint.

Review of literature [1- 15] indicated that simulation of physical vapor deposition process of Tantalum carbide on 316L SS is not yet reported. This paper was aimed at investigating the effect of physical vapor deposition (PVD) parameters such as vacuum pressure, argon gas velocity and substrate stand-off-distance on mass concentration and turbulence kinetic energy of Argon gas in a sputtering chamber.

2.0 Geometric Modeling

Sputtering chamber was modelled using SOLID WORKS V15. Solid modelling tool was used to create a circular chamber with diameter of 55 mm cross section as shown in Fig. 1. The chamber has provisions to place three substrates. Substrate Inlet 1 location at 15 mm from chamber inlet was created. After creating a substrate inlet 1, other two substrates were created at 45 mm and 80 mm from the inlet. A substrate pan width of 5 mm was created in-side the substrate. Split command was used to generate the solid section with the chamber dimensions. After creating a substrate-1, pattern command was used to create other two substrates with even spacing.

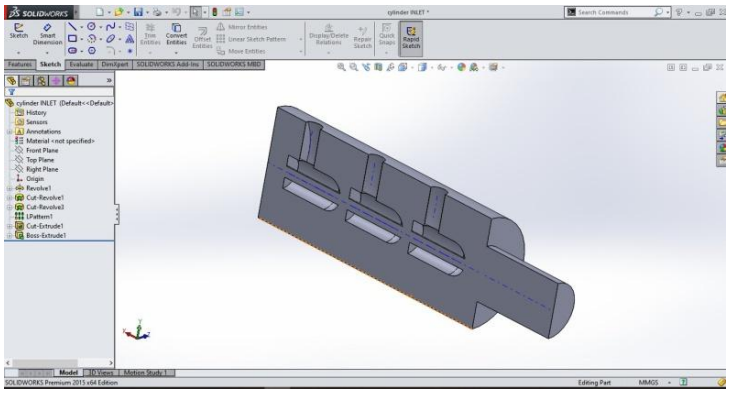

Fig. 1 Chamber section model with substrates

3.0 Computational Fluid Dynamics Analysis

ANSYS Fluent and ICEM CFD meshing were used for the study. Fluent was selected because of it facilitates simulations in both 2D and 3D. ICEM CFD meshing was selected for the large degree of control that it allows the user when creating and refining the mesh. Meshing was manually performed as the geometry was simple to produce a high-

quality mesh with a low element count. In addition to the three substrates, an extra volume was suggested to represent the evaporation of Ar gas: an area above the substrate that would serve as the source region for introducing Ar gas into the system. The model was exported from SolidWorks as a para-solid file and imported to ANSYS. The part names for each geometry element were assigned using ICEM CFD depending on the boundary condition it represented.

A pre-mesh (Fig. 2) was developed once the whole association was made, and the mesh was checked for association errors. The ICEM CFD edge property management tools were used to regulate the mesh size. By linking the edges of adjacent sections and setting the transition ratio to 1.2 instead of the default 2, a seamless transition between regions of varying element density was accomplished. The mesh was exported to FLUENT for setup and simulation after boundary condition types were assigned to each part of the model.

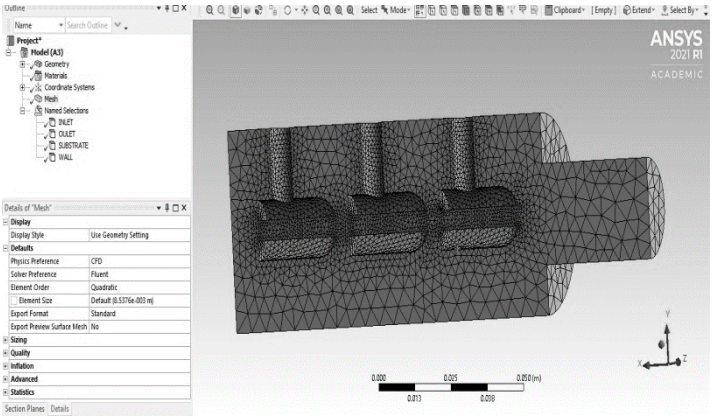

Fig. 2 Meshing of PVD sputtering chamber model

The meshed models were exported to ANSYS FLUENT for further analysis. The simulation conditions considered for the analysis is shown in Table 1 at normal operating conditions. For continuity, moment, and energy equations, SIMPLE pressure-velocity coupling was adopted, and second order discretization schemes were applied.

Table 1. Simulation conditions used for analysis of the Sputtering Chamber

Pressure(Pa)	Velocity (mm/s)	Sputter stand-off-distance
0.41	3.40	10
0.48	6.78	45
0.57	13.57	80

The main factors of CFD simulation were thermal conditions, evaporation of metal and its mixing with carrier gas. The energy equation and species transfer were included to the model. The solid material attributes were obtained from ANSYS material library. Properties of the fluids were obtained from other sources. The ideal gas hypothesis is appropriate for modelling the process including low pressures and high temperatures. This was not invoked to compute fluid densities for simulation simplicity. Wall boundary condition was applied to all the walls, and the symmetry boundary condition was applied to the Z-Y plane. The entry, exit, and wall boundary criteria were the four most critical boundary conditions. Fig. 3 shows the boundary condition applied to the chamber model. According to the experimental setup, the entry and exit boundary conditions were selected. At both the input and the outflow, pressure boundary conditions were applied. Precise values were selected based on the pressure measured at the intake of the chamber and outflow throughout the experiment. Two sets of boundary conditions were created. On the basis of experimental observations, the inlet temperature was set to room temperature, and zero mass fraction was imposed at the inlet for Ar entering the chamber. The model setup and solution initialization (Fig. 3) are flexible with respect to defining the initial Ar gas velocity in X, Y and Z directions with turbulent kinetic energy at different substrate locations and specific dissipation rate being constants automatically updated by the software

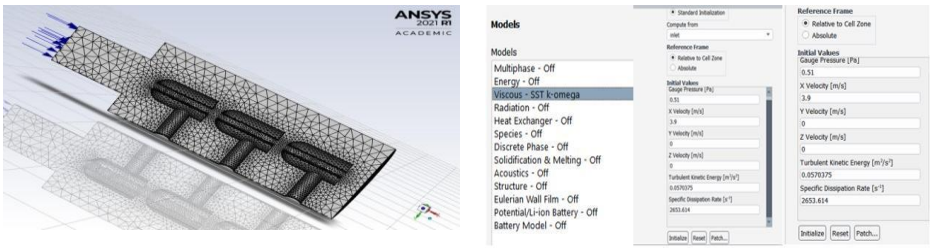

Fig. 3 Boundary conditions applied to meshed model
(Input, output and wall boundary Conditions)

A plane at the mid span of the chamber is created as shown in Fig. 4. This cut plane is used to obtain the mass concentration plots and turbulence kinetic energy along the vacuum sputtering chamber. After simulating the flow conditions the results were obtained using CFD Post Software by defining the plane required for results. A plane is selected at the mid span of the sputtering chamber.

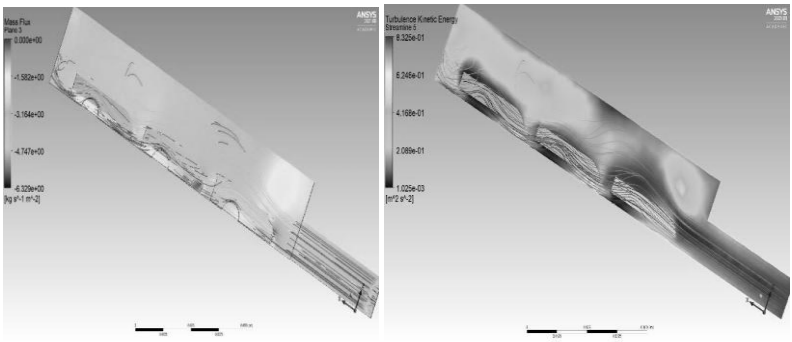

Fig. 4 CFD Post processing images

4.0 Results and Discussion

Process flow parameters such as vacuum pressure, Ar velocity, stand-off-distance plots for all the models as per L_{27} array were studied with initial approximations and iterations (Fig. 5). Residual plot of velocity streams for Ar gas flow along the sputter chamber reveals that for a count of 50 iteration trials, the velocity drops along the chamber as the area increases with as a reasonable starting point. As Residual plot converges the simulation for the iteration of 50 for the input residuals. The input argon (Ar) gas velocity and pressure parameters have converged around 50 iterations, according to the results. The plot for the amount of interest, as well as the convergence plot, are both converged.

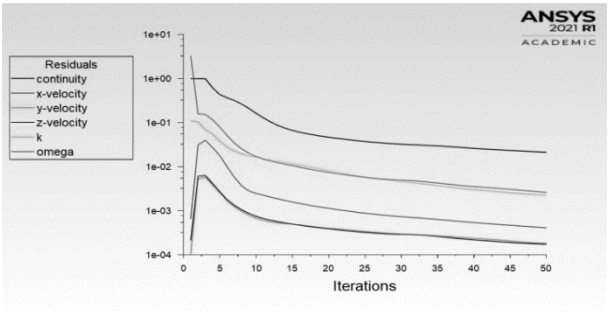

Fig. 5 Residuals for velocity and turbulence characteristics

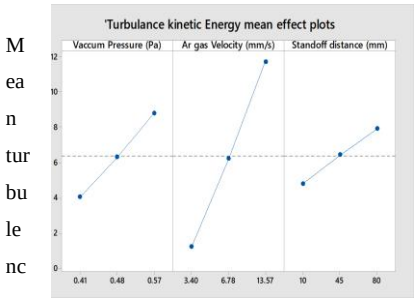

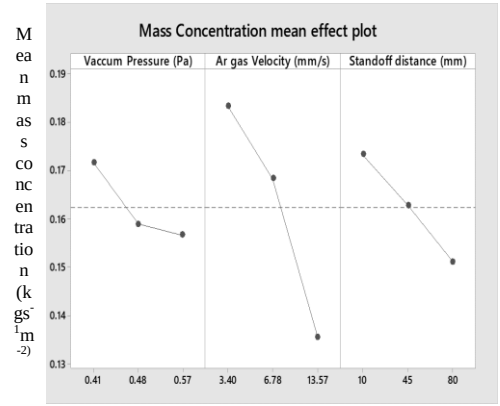

Fig. 6 Main effect plots for **a)** mass concentration and **b)** turbulence energy

For increase in vacuum pressure, Ar gas velocity and stand-off-distance, decrease in mean Ar gas mass concentration was observed (Fig. 6). This is because with decrease in vacuum pressure the chamber becomes more ideal and free from other gases except Ar gas. Thus, as vacuum pressure increases the chamber gets contaminated with external gases and Ar gas mass concentration decreases. At higher Ar velocity, its residence time in the chamber decreases. At higher velocity the ion bombardment is faster. Standoff distance is the distance between vacuum chamber gas inlet and substrate. As the distance between the two increases the area between the two gets widened and mass concentration becomes weak. Amongst the three parameters, increase in Ar gas velocity from 3.40 mm/s to 13.57 mm/s caused significant decrease in mass concentration from 0.1833 $kgs^{-1}m^{-2}$ to 0.1356 $kgs^{-1}m^{-2}$. As shown in Fig.6, turbulence kinetic energy increased with increase in all the three parameters. With increase in vacuum pressure, the chamber gets affected by other atmospheric gases and turbulence energy inside the chamber increases. Ar gas velocity directly influences turbulence effect in the chamber. As stand-off-distance increases the ion bombardment gets delayed resulting in increase of turbulence kinetic energy.

5.0 Conclusion

The sputtering chamber was modelled with standard specification and analyzed using ANSYS CFD Fluent and parametric study was performed using L_{27} array. Based on the simulation results, conclusions were arrived at:

Optimal vacuum pressure, Ar gas velocity and stand-off-distance were 0.41Pa, 3.4 mm/s and 10 mm respectively. Maximum mass concentration was 0.1009 $kgs^{-1}m^{-2}$ and minimum turbulence energy was 0.1968 m^2s^{-2}.

The streamline plots showed appreciable change in Ar gas velocity along the chamber. It has positive effect near the entry of the chamber at 10 mm stand-off- distance.

ANOVA results showed that all the three parameters: vacuum pressure, Ar velocity and stand-off- distance were significant for mass concentration and turbulence.

Turbulence kinetic energy increased with increase in all the three parameters. With increase in the three parameters, vacuum pressure the chamber decreased.

References

1. J M Kapopara, A R Mengar, K V Chauhan, N P Patel, S K Rawal, Modelling and analysis of sputter deposited ZrN coating by CFD, *In IOP Conference Series: Materials Science and Engineering,* 149 (1), 012205, 2016
2. M V P Kumar, I Bhanulatha, Design and structural analysis of knee implants using different materials, *International Journal Of Advance Scientific Research and Engineering Trends,* 5 (7), 32-38, 2020
3. Z Ziyu, Simulation of the mechanical and flow behaviour of bone fixation implants, dissertation, Imperial College London (PhD thesis), 2013
4. A Baptista, F Silva, J Porteiro, J Míguez, G Pinto, Sputtering physical vapour deposition (PVD) coatings: A critical review on process improvement and market trend demands, *Coatings,* 8 (11), 402, 2018
5. F J Jimenez, S K Dew, Comprehensive computer model for magnetron sputtering. I. Gas heating and rarefaction, *Journal of Vacuum Science & Technology A: Vacuum, Surfaces, and Films,* 30 (4), 041302, 2012
6. H Hoche, S Groß, M Oechsner, Development of new PVD coatings for magnesium alloys with improved corrosion properties, *Surface and Coatings Technology,* 259, 102-108, 2014
7. R Manivannan, S Sundararaj, R Dheenasagar, K Giridharan, P R Sivaraman, V Udhayarani, Influence of Al_2O_3, SiC and B_4C covalent multilayer PVD coating on surface properties of HSS rod, *Materials Today: Proceedings,* 39, 700-707, 2021
8. H Kitajima, M Hirota, T Iwai, K Hamajima, R Ozawa, Y Hayashi, Y Yajima, M Iida, T Koizumi, M Kioi, K Mitsudo, T Ogawa, Computational fluid simulation of fibrinogen around dental implant surfaces, *International journal of molecular sciences,* 21 (2), 660, 2020

9. V Varghese, Finite element based of hip joint prosthesis, National Institute of Technology, Rourkela, Orissa (MTech Thesis), 2011
10. R Alias, R Mahmoodian, M H A Shukor, Development and characterization of a multilayer silver/silver-tantalum oxide thin film coating on stainless steel for biomedical applications, *International Journal of Adhesion and Adhesives*, 92 (4), 89-98, 2019
11. T Kobayashi, Monte Carlo simulation of gas transport in a TiN reactive sputtering apparatus for large area deposition, *Vacuum*, 74 (3-4), 379-385, 2004
12. D Nakamura, A Suzumura, K Shigetoh, Sintered tantalum carbide coatings on graphite substrates: Highly reliable protective coatings for bulk and epitaxial growth, *Applied Physics Letters*, 106, 082108, 2015
13. J M Kapopara, A R Mengar, K V Chauhan, S K Rawal, CFD analysis of sputtered TiN coating, *Materials Today: Proceedings* 4 (9), 9390-9393, 2017
14. G Pinto, F J G Silva, J Porteiro, J L Miguez, A Baptista, L Fernandes, A critical review on the numerical simulation related to physical vapour deposition, *Procedia Manufacturing*, 17 860-869, 2018
15. H Fouad, In vitro evaluation of stiffness graded artificial hip joint femur head in terms of joint stresses distributions and dimensions: finite element study, *Journal of Materials Science: Materials in Medicine*, 22 (6), 1589-1598, 2011